Radiol Phys Technol (2013) 6:202–209
DOI 10.1007/s12194-012-0189-7

Automated adjustment of display conditions in brain MR images: diffusion-weighted MRIs and apparent diffusion coefficient maps for hyperacute ischemic stroke

Hiroyuki Nagashima · Kunio Doi · Toshihiro Ogura · Hiroshi Fujita

Received: 17 September 2012 / Revised: 7 November 2012 / Accepted: 15 November 2012 / Published online: 27 November 2012

Abstract We developed a new computerized scheme for proper display of brain diffusion-weighted magnetic resonance images (DWIs) and apparent diffusion coefficient (ADC) maps based on density histogram analysis. In our scheme, DWI volumes and *b*0 image volumes of 44 cases were first created, and brain regions on DWI volumes were segmented. ADC map volumes were then derived from both volumes. The density histogram was determined from the brain regions on these volumes, and the voxel value corresponding to the maximum in the density histogram was determined for each volume. The display gray level for each of the two volumes was adjusted by setting the determined voxel value as window conditions. In a comparison between the existing manual method and our automated method, the variation in the gray levels was evaluated quantitatively. The variation in the average of the cross-correlation values determined for pairs of density histograms in each of the DWIs and ADC maps was 57.3 and 27.1 % with the existing method, respectively, and 7.7 and 2.7 % with our scheme, respectively, which indicated a more consistent display of images with our scheme. The performance of the two-alternative-forced-choice method for visual comparison of pairs of images in each of the DWIs and ADC maps adjusted by our scheme was judged to be better than those of the existing method by 75.1 % and 92.7 %, respectively. Our computerized scheme would be a promising technique for an accurate, prompt automated adjustment of display conditions in brain DWIs and ADC maps.

Keywords Computerized scheme · Diffusion-weighted magnetic resonance image · Apparent diffusion coefficient maps · Acute ischemic stroke · Display condition adjustment

H. Nagashima (✉) · K. Doi · T. Ogura
School of Radiological Technology, Gunma Prefectural College of Health Sciences, 323-1 Kamioki-machi, Maebashi, Gunma 371-0052, Japan
e-mail: nagashima@gchs.ac.jp

K. Doi
Department of Radiology, The University of Chicago, 5841 South Maryland Avenue, Chicago, IL 60637, USA

H. Fujita
Division of Regeneration and Advanced Medical Sciences, Department of Intelligent Image Information, Graduate School of Medicine, Gifu University, 1-1 Yanagido, Gifu, Gifu 501-1194, Japan

1 Introduction

In diagnostic imaging of hyperacute ischemic stroke, computed tomography (CT) can show subtle image findings of the initial stage of cerebral ischemia. However, subtle findings that appear on brain CT images within 6 h of the occurrence of symptoms could be overlooked if the CT images are not interpreted carefully; the recognition accuracy varies with the observer's experience [1]. On the other hand, diffusion-weighted magnetic resonance images (DWIs) can clearly demonstrate the ischemic regions, and they can identify ischemic regions much better than can CT in both detection sensitivity and observer agreement [2, 3]. Moreover, apparent diffusion coefficient (ADC) maps derived from the DWIs and concurrent images (*b* value = 0: *b*0 image) are used for deciding whether the high-intensity regions on DWIs are due to T2 shine-through phenomena or due to the diffusion restriction [4–6]. The degree of signal intensity and the range of cerebral ischemia in these images can provide important information for decisions regarding treatment strategy [7–11]. However, this image information

can change substantially depending on the display conditions such as the window level and width [12]. Therefore, observing DWIs and ADC maps under improper image display conditions may result in detection errors for localized lesions and inaccurate delineation of the ischemic range.

As a solution for these problems, the standardization method of setting the image display conditions for DWIs, which is determined by use of the signal intensity of the thalamus in a *b*0 image, was proposed by the Acute Stroke Imaging Standardization Group in Japan (ASIST-Japan) [13–15]. Recent reports by ASIST-Japan indicated that this method can decrease the variation of DWI display conditions among institutions and operators. However, the proposed method is time consuming, because the selection of the region of interest (ROI) in the thalamus must be done manually by operators. Moreover, the incidence of intracerebral hemorrhage and lacunar infarction is greater for the thalamus than for other organs [16], and when a circular ROI is selected for the location, including these diseases in a *b*0 image, the signal intensity and image contrast in DWIs may change greatly. In addition, even if an ROI is selected for a location outside the lesions in the thalamus by reduction of the ROI size to avoid such an issue, the variation in display conditions can be very large due to inadequate sampling of image data.

To compensate for these shortcomings with the method proposed by ASIST-Japan, we have developed a computerized scheme [17] that can automatically adjust the display conditions in DWIs using the pixel value corresponding to the maximum determined from the density histogram for the brain regions in *b*0 images. Consequently, the signal intensity and image contrast of DWIs obtained by the computerized method were visually more similar than those obtained by the ASIST-Japan-based manual method.

In this study, we developed a new computerized scheme, without using the *b*0 images for proper display of DWIs, which is based on analysis of the density histogram. In diagnostic imaging and treatment decisions for hyperacute ischemic stroke, although not only DWIs but also ADC maps are used effectively, the study of the standardization of display conditions for ADC maps has not been reported previously, even by ASIST-Japan. Therefore, we also developed a computerized scheme for automated adjustment of display conditions in ADC maps.

2 Materials and methods

2.1 Image database

In this study, we used DWIs and *b*0 images from 44 cases, which were obtained within the first 6 h after stroke onset, with use of two 1.5 T MRI scanners (Genesis Signa and Signa Excite, GE Healthcare, Milwaukee/WI/USA). These images were obtained from 29 men and 15 women (age range 22–89 years, mean age 66.9 ± 14.9 years). Our institutional review board approved the use of this image database for this study. For the scanning conditions, the spin-echo echo-planar imaging (SE-EPI) sequence was chosen, and the scan parameters were set as follows: repetition time = 5000–10000 ms, echo time = 86–102 ms, flip angle = 90°, slice thickness = 5 mm, and motion-probing gradient (MPG) = 3 directions. The variation in the repetition time and echo time was large because this image database was created with images obtained at two institutions (Kiryu Kosei General Hospital and Central Gunma Neurosurgical Hospital) where the scan parameters were different. Both images were obtained from 16 to 24 slices (mean 21.2 ± 2.3 slices) per case, depending on the range of scanning.

2.2 Creation of volume data

The overall computerized scheme for automated adjustment of display conditions in brain DWIs and ADC maps is shown in Fig. 1. In our computerized scheme, the original brain DWIs and *b*0 images [matrix size 256 × 256, gray-scale 12 bits, pixel size (field of view): 0.820–0.937 mm (210–240 mm)] were entered into a computer, and the volume data were produced by combining all of the slices in each of the two images.

2.3 Segmentation of brain regions and creation of ADC map volumes

For segmenting of the initial brain regions, DWI volumes were first binarized by means of a thresholding technique,

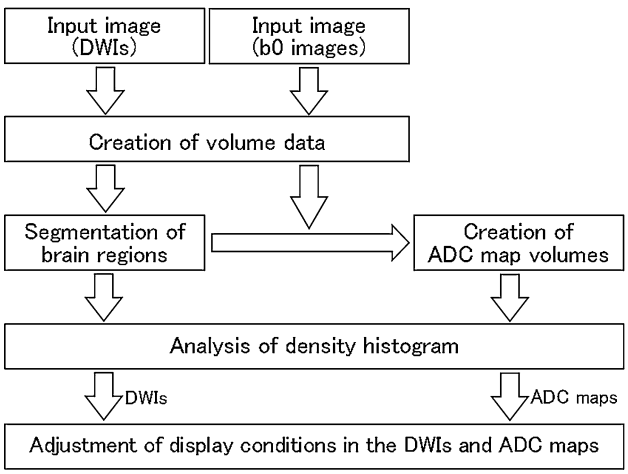

Fig. 1 Overall computerized scheme for automated adjustment of display conditions for brain DWIs and ADC maps

which is based on discriminant analysis [18]. The candidates were then identified in the binarized volumes, and the obvious noise was removed by setting of a threshold of 1 % as the ratio of the identified candidate volumes to the image volumes. Finally, the brain regions on the DWI volumes were segmented by use of reverse processing of gray-level, labeling, and erosion/dilation techniques. Figure 2 shows an example of (a) a slice of original DWIs, (b) its initial binary image by use of a thresholding technique, (c) its binary image of brain regions after labeling and morphologic processing applied to image (b), and (d) a slice of the ADC map volume. The ADC map volumes [19] were derived based on the signal intensity at each voxel in segmented brain regions of the *b*0 image volumes and the original DWI volumes together with the strength of the MPG. In addition, the strength of the MPG of the *b*0 images and the DWIs was set to 0 and 1000 s/mm^2, respectively.

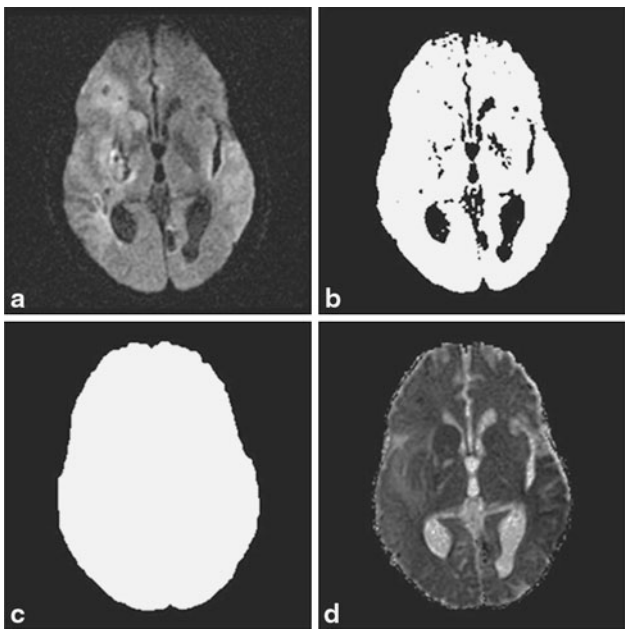

Fig. 2 Segmentation of brain images: **a** DWI, **b** binary image by use of a thresholding technique based on discriminant analysis, **c** binary image of brain regions with labeling and morphologic processing, and **d** ADC map of brain regions with labeling and morphologic processing

2.4 Analysis of density histogram

An important part of our algorithm is density histogram analysis, to adjust the gray level of brain DWIs and ADC maps. In a previous study [20], we adopted the method of using a CT value of the maximum frequency in the density histogram to normalize the gray level in the CT images which may differ among cases and scanners. As a result, highly accurate processing was achieved. For this reason, we also applied this method for proper adjustment of the display conditions of MR images in the present study.

Figure 3 illustrates our method on a density histogram for analysis of the brain regions in DWI volumes. The density histogram (see Fig. 3a) was first determined for the entire brain regions in each of the original DWI volumes and the ADC map volumes. The density histogram included commonly the mixture of the voxel values corresponding to both normal and abnormal regions.

We removed abnormal areas in the density histogram determined from DWI volumes using the variable thresholding technique [21] (see threshold in Fig. 3a). Next, the density histogram for normal brain regions in each of the two volumes was smoothed by use of the simple moving-average method in every 20 sections on the voxel values (see Fig. 3b), because the variation among frequencies for each voxel value on the initial density histogram can influence the determination of a voxel value corresponding to the maximum frequency. In addition, the number of sections for the simple moving average was optimized for each case by examination of the variation in the voxel value corresponding to the maximum in the density histogram by changes in the number of sections from 5 to 30. Finally, the voxel value corresponding to the maximum frequency in the density histogram was determined from the smoothed density histogram for each volume (see Fig. 3b).

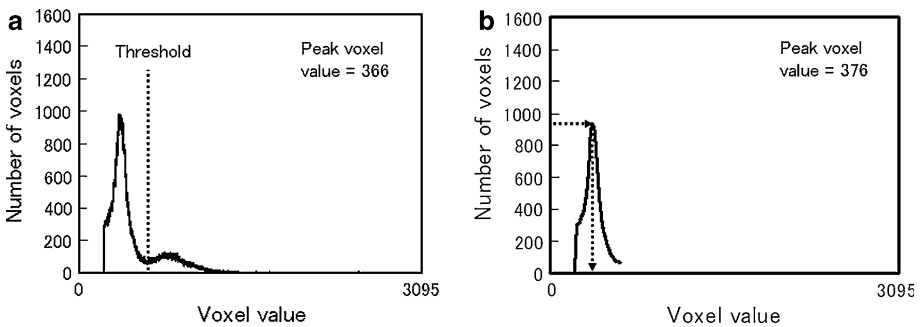

Fig. 3 Illustration of our method for analysis of density histogram of DWI volumes: **a** initial density histogram determined from the entire brain regions where voxel values above the threshold corresponding to an abnormal region are removed, **b** smoothed density histogram only for normal brain region

2.5 Adjustment of display conditions in the DWIs and ADC maps

We adjusted the display conditions for DWI volumes by defining the voxel value corresponding to the maximum frequency as a window center, and two times the voxel value as a window width (WW), whereas the display conditions for ADC map volumes were adjusted by determination of three times the voxel value as a window center, and two times the window center as a WW. These window conditions were determined empirically so that the signal intensity and image contrast of both volumes adjusted by our computerized scheme would match to the gray level of each volume adjusted by the manual methods as much as possible.

In addition, the grayscale for both volumes was converted into eight bits with the equation

$$g(i,j,z) = 255 \times \frac{f(i,j,z)}{\mathrm{WW}} \tag{1}$$

where the functions $g(i, j, z)$ and $f(i, j, z)$ are the signal intensity at each voxel of the converted volumes and the original volumes, respectively. When $g(i, j, z)$ was larger than 255, the voxel value was set to 255.

2.6 Evaluation of our computerized scheme

2.6.1 Voxel values corresponding to the maximum and full width at half maximum in the density histogram

For quantitative evaluation of the signal intensity and image contrast, we used two parameters, namely, the voxel value (H_{P}) corresponding to the maximum determined from the density histogram and the voxel value (H_{W}) corresponding to the full width at half maximum in the density histogram for DWI volumes and also for the ADC map volumes.

With the consensus of two neurosurgeons, the manual method by ASIST-Japan with use of 44 cases of brain DWIs and $b0$ images was first performed; manual adjustment of the display conditions by use of ADC maps created by this study was also performed. The grayscales of the original DWI volumes and the ADC map volumes were then converted separately by use of the WW determined by the manual method. Finally, the density histogram was determined from the brain regions in each of the two volumes converted by the manual method and our computerized method, and the H_{P} and the H_{W} were obtained. In a comparison between the manual method and our computerized method for each of the DWIs and ADC maps, the variation in the H_{P} and H_{W} was evaluated among cases.

2.6.2 Cross-correlation for density histogram

Cross-correlation (CC) has been applied to the evaluation of the shape similarity in pattern recognition and registration among images [22, 23]. In this study, to evaluate the variation in the signal intensity and image contrast among cases, we determined the CC for the density histogram of the converted volumes concerning the shape of the density histogram.

We first prepared 20 cases randomly selected from the 44 cases of DWIs and ADC maps adjusted by two different methods. The CC values for the density histogram in the brain regions for 190 pairs of all combinations obtained from the 20 cases were then determined from the equation

$$\mathrm{CC} = \frac{1}{B}\sum_{B=0}^{B-1}\frac{(f-\overline{f})(g-\overline{g})}{\sigma_f \sigma_g} \tag{2}$$

where B is the grayscale in eight bits, f and g are the frequencies of each voxel value of the density histogram in the brain regions for each of the pairs, $\overline{f}$ and $\overline{g}$ are the averages, and σ_f and σ_g are the standard deviations. In a comparison between the manual and computerized methods for each of the DWIs and ADC maps, the variation in the CC values among the 190 pairs was evaluated.

2.6.3 Two-alternative-forced-choice (2-AFC) study for visual evaluation of similarity of displayed images

We also performed a 2-AFC study using the 190 pairs of DWIs and of ADC maps adjusted by manual and computerized methods. The observers were five radiologists with 9–29 years of experience (mean experience 14.6 ± 8.2 years). Before the observer study, we provided a summary of the study and explained the evaluation procedure to the observers. For the 2-AFC method, the 190 pairs adjusted by two different methods were displayed side by side on a liquid–crystal display (LCD) monitor, which is illustrated in Fig. 4. We asked the observers to evaluate the subjective similarity of the signal intensity and image contrast in the brain regions for pairs of DWIs and of ADC maps, and to select the more similar pair by comparing the pairs of images adjusted by the two different methods. In comparison between the methods for each of the DWIs and ADC maps, the selection rate of each method in the 190 pairs was determined.

3 Results

The average and the standard deviation of the H_{P} obtained from the density histograms in DWIs and ADC maps for

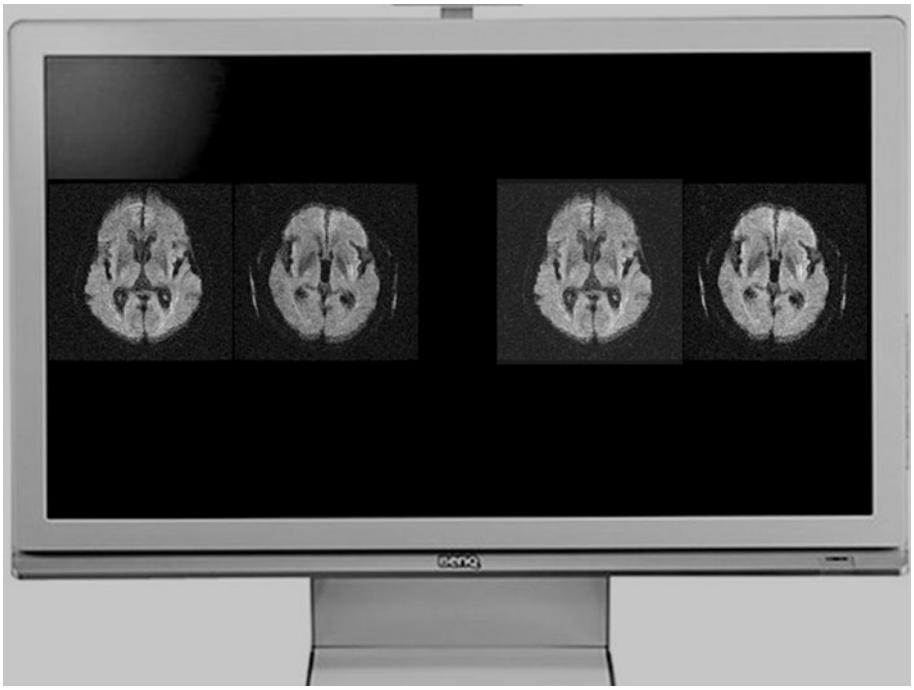

Fig. 4 Illustration of two pairs of selected images on an LCD monitor for 2-AFC studies by use of DWIs adjusted by the manual method (*right*) and our computerized scheme (*left*). The position (*right* or *left*) was selected randomly for each case

Table 1 Comparison of the manual method and the computerized scheme for the average and the standard deviation of the peak voxel value (H_P) obtained from density histograms in each of the DWIs and ADC maps for 44 cases

	Manual method	Computerized method
DWI		
Average	112.5	127.2
Standard deviation	14.9 (13.2 %)	1.4 (1.1 %)
ADC map		
Average	50.6	46.6
Standard deviation	7.2 (14.2 %)	1.2 (2.6 %)

Table 2 Comparison of the two methods for the average and the standard deviation of the histogram width (H_W) obtained from density histograms in each of the DWIs and ADC maps for 44 cases

	Manual method	Computerized method
DWI		
Average	39.9	44.7
Standard deviation	10.3 (25.8 %)	5.5 (12.4 %)
ADC map		
Average	46.6	42.7
Standard deviation	9.6 (20.6 %)	6.3 (14.9 %)

the 44 cases based on the manual methods and on the computerized scheme are shown in Table 1. With the existing manual method (ASIST-Japan), the variation in H_P for the 44 cases for the signal intensity determined from the DWIs was 13.2 %, and it was 1.1 % with our computerized method. For the ADC maps, the variation in H_P was 14.2 % with the existing method, and 2.6 % with our method. The standard deviations between the two methods for H_P determined for each case in the DWIs and ADC maps were significantly different ($p < 0.001$). Thus, our computerized method can display more consistent images than can the manual method.

The average and the standard deviation of the H_W obtained from density histograms in the DWIs and ADC maps for the 44 cases based on the two methods are shown in Table 2. With the existing method, the variation in H_W for image contrast in the DWIs was 25.8 and 12.4 % with our method. The variation in H_W for ADC maps with the existing method was 20.6 and 14.9 % with our method. The standard deviations between the two methods for H_W, determined for each case in the DWIs and ADC maps, differed significantly ($p < 0.001$ and $p < 0.01$, respectively). Thus, this result indicated a more consistent display of images with our computerized method.

The average and the standard deviation of the CC values determined from density histograms in each of the DWIs and ADC maps for the 190 pairs of 20 cases based on the two methods are indicated in Table 3. The variation in CC values for DWIs was 57.3 % with the existing method, and 7.7 % with our method. The variation in CC values for ADC maps was 27.1 % with the existing method, and 2.7 % with our method. The statistical significance of the difference in the standard deviations between the two methods for the CC value was determined for each pair of DWIs and ADC maps. As a result, the two differed significantly, with a p value for both that was <0.001. These

Table 3 Comparison of the two methods for the average and the standard deviation of the cross-correlation (CC) value determined from density histograms in each of the DWIs and ADC maps for 190 pairs of 20 cases

	Manual method	Computerized method
DWI		
Average	0.572	0.900
Standard deviation	0.328 (57.3 %)	0.070 (7.7 %)
ADC map		
Average	0.751	0.936
Standard deviation	0.212 (27.1 %)	0.025 (2.7 %)

Table 4 Comparison of the two methods for the selection rate obtained by 2-AFC studies for the subjective similarity of pairs of images in each of the DWIs and ADC maps

Observer	Manual method (%)	Computerized method (%)
DWI		
A	24.2	75.8
B	29.5	70.5
C	24.2	75.8
D	25.8	74.2
E	21.1	78.9
Average	24.9	75.1
ADC map		
A	6.3	93.7
B	8.4	91.6
C	4.7	95.3
D	11.6	88.4
E	5.3	94.7
Average	7.3	92.7

results suggest that our computerized scheme can provide a more consistent display compared with existing manual methods.

The selection rate obtained by 2-AFC studies for the subjective similarity of pairs of displayed images in each of the DWIs and ADC maps based on the two methods is shown in Table 4. The selectivity for pairs of images in the DWIs and ADC maps adjusted by use of our computerized scheme showed larger values for all observers, and the mean value among observers was 75.1 and 92.7 %, respectively. Thus, it seems clear that our computerized method can display more similar brain images than can the manual method.

Figures 5 and 6 show three cases of brain DWIs and ADC maps, respectively, adjusted by the two different methods. The upper images (a, b, and c) were obtained by the manual method, and the lower images (d, e, and f) were obtained by our computerized scheme. In the DWIs and ADC maps adjusted by the existing manual method (ASIST-Japan) and by neurosurgeons, the gray levels in the normal brain regions were different visually among cases, and were not consistent. On the other hand, the signal intensity and image contrast of images in all cases obtained by our computerized method in DWIs and ADC maps were more similar than those obtained by the manual method. This result shows that our computerized scheme based on the density histogram analysis can be used for reduction of the variation of gray levels among cases in brain DWIs and ADC maps.

4 Discussion

The gray levels in each of the brain DWIs and ADC maps are known to differ among vendors and subjects, and also to change depending on static magnetic fields and scanning conditions [24]. Therefore, the gray levels in the DWIs and ADC maps cannot be used for the quantitative evaluation, and thus the ratio of average gray levels in an abnormal region and the contralateral normal region for the median-sagittal line of the brain has been applied for the decision on the reversibility of brain ischemic regions by use of ADC maps [25, 26]. In this study, we determined the gray level corresponding to the maximum for each of the DWIs and ADC maps based on density histogram analysis, and then converted the grayscale for both images using these gray levels. In addition, the variation in the gray levels on converted images was determined. Consequently, the variation in the gray levels of both images obtained by our method has decreased significantly among cases compared with that obtained by existing methods. With this computerized scheme, we can normalize the gray levels in the DWIs and ADC maps which may differ among vendors and subjects. Thus, it would be possible to evaluate quantitatively the normalized ischemic regions in the DWIs and ADC maps using our computerized method.

In the present study, it was suggested that our computerized scheme can provide a more consistent display compared with existing manual methods. However, verification of clinical usefulness with our computerized scheme will be required in the future. In particular, it will be important to make a clinical assessment on localized lesions with different display methods by carrying out an observer performance study using both images adjusted by the existing manual method and our automated method.

The central processing unit (CPU) time for processing required for this computerized scheme was about 7.0 s per case with our computer (Pentium D, CPU 3.60 GHz). This result indicates that observers could interpret brain DWIs and ADC maps accurately and promptly using the computerized scheme without complicated and time-consuming manual adjustment of the display conditions, such as

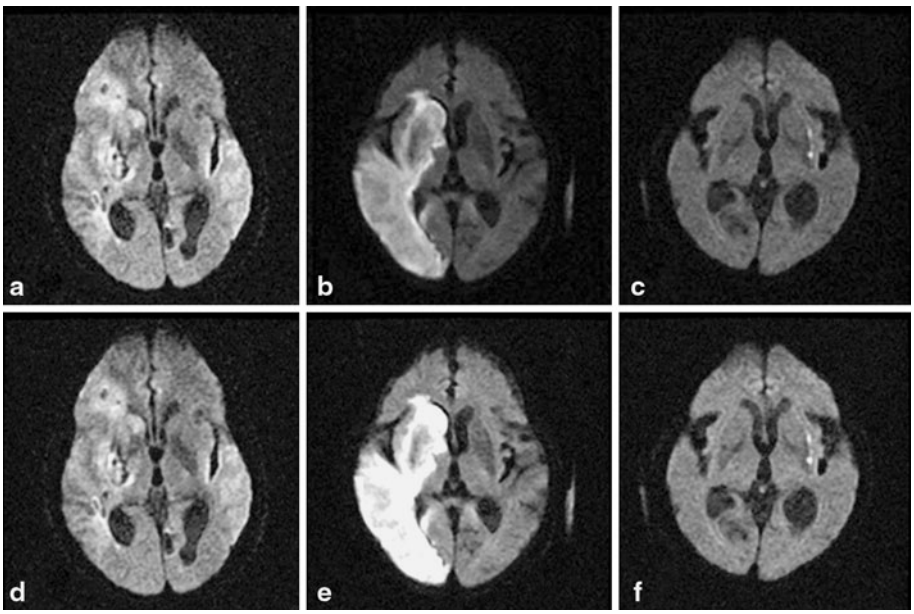

Fig. 5 Illustration of three cases of brain DWIs adjusted by the existing manual method in **a**, **b**, and **c**, and by our computerized scheme in **d**, **e**, and **f**. Note the uniform and consistent display of these brain images by our computerized scheme in terms of the image brightness and contrast

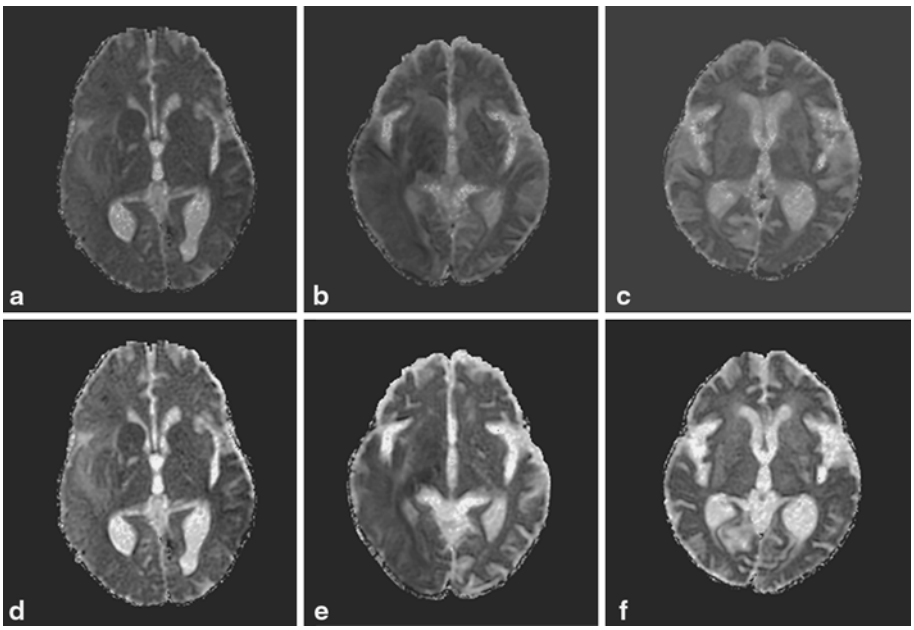

Fig. 6 Illustration of three cases of brain ADC maps adjusted by neurosurgeons in **a**, **b**, and **c**, and by our computerized scheme in **d**, **e**, and **f**. Note the uniform and consistent display of these brain images by our computerized scheme in terms of the image brightness and contrast

the window level and width. This computerized scheme using density histogram analysis is therefore a promising technique for automated adjustment of the display conditions in brain DWIs and ADC maps, and it would be useful for radiologists and neurosurgeons for (1) preventing incorrect decisions due to artifacts, (2) reducing the variation in decisions about the ischemic range, and (3) achieving a proper assessment of thrombolytic therapy.

Acknowledgments The authors are grateful to the Departments of Radiology, Kiryu Kosei General Hospital and Central Gunma Neurosurgical Hospital, for providing the image data. This work was supported by Japan Society for the Promotion of Science (JSPS) KAKENHI Grant Number 23591784.

References

1. Kalafut Ma, Schriger DL, Saver JL, Starkman S. Detection of early CT signs of >1/3 middle cerebral artery infarctions: interrater reliability and sensitivity of CT interpretation by physicians involved in acute stroke care. Stroke. 2000;31(7):1667–71.
2. Saur D, Kucinski T, Grzyska U, Eckert B, Eggers C, Niesen W, Schoder V, Zeumer H, Weiller C, Röther J. Sensitivity and interrater agreement of CT and diffusion-weighted MR imaging

in hyperacute stroke. AJNR Am J Neuroradiol. 2003;24(5): 878–85.
3. Barber PA, Hill MD, Eliasziw M, Demchuk AM, Pexman JH, Hudon ME, Tomanek A, Frayne R, Buchan AM. Imaging of the brain in acute ischaemic stroke: comparison of computed tomography and magnetic resonance diffusion-weighted imaging. J Neurosurg Psychiatry. 2005;76:1528–33.
4. Burdette JH, Elster AD, Ricci PE. Acute cerebral infarction: quantification of spin-density and T2 shine-through phenomena on diffusion-weighted MR images. Radiology. 1999;212(2):333–9.
5. Provenzale JM, Engelter ST, Petrella JR, Smith JS, MacFall JR. Use of MR exponential diffusion-weighted images to eradicate T2 "shine-through" effect. AJR Am J Roentgenol. 1999;172(2): 537–9.
6. Siemonsen S, Mouridsen K, Holst B, Ries T, Finsterbusch J, Thomalla G, Ostergaard L, Fiehler J. Quantitative t2 values predict time from symptom onset in acute stroke patients. Stroke. 2009;40(5):1612–6.
7. van Everdingen KJ, van der Grond J, Kappelle LJ, Ramos LM, Mali WP. Diffusion-weighted magnetic resonance imaging in acute stroke. Stroke. 1998;29(9):1783–90.
8. Lansberg MG, Thijs VN, O'Brien MW, Ali JO, de Crespigny AJ, Tong DC, Moseley ME, Albers GW. Evolution of apparent diffusion coefficient, diffusion-weighted, and T2-weighted signal intensity of acute stroke. AJNR Am J Neuroradiol. 2001;22(4):637–44.
9. Montiel NH, Rosso C, Chupin N, Deltour S, Bardinet E, Dormont D, Samson Y, Baillet S. Automatic prediction of infarct growth in acute ischemic stroke from MR apparent diffusion coefficient maps. Acad Radiol. 2008;15(1):77–83.
10. Nezu T, Koga M, Naganuma M, Kimura K, Shiokawa Y, Nakagawara J, Furui E, Yamagami H, Okada Y, Hasegawa Y, Kario K, Okuda S, Minematsu K, Toyoda K. Pre-treatment ASPECTS-DWI score has a relation with functional outcome at 3 months following intravenous rt-PA therapy (in Japanese). Jpn J Stroke. 2009;31:366–73.
11. Bråtane BT, Bastan B, Fisher M, Bouley J, Henninger N. Ischemic lesion volume determination on diffusion weighted images vs. apparent diffusion coefficient maps. Brain Res. 2009; 7:182–8.
12. Hirai T, Sasaki M, Maeda M, Ida M, Katsuragawa S, Sakoh M, Takano K, Arai S, Hirano T, Kai Y, Kakeda S, Murakami R, Ikeda R, Fukuoka H, Sasao A, Yamashita Y. Diffusion-weighted imaging in ischemic stroke: effect of display method on observer's diagnostic performance. Acad Radiol. 2009;16(3):305–12.
13. Sasaki M, Fujiwara S. Clinical diffusion-weighted MRI for cerebral disorders: current concepts (in Japanese). Jpn Ger Med Rep. 2005;50(4):621–8.
14. Sasaki M. Standardization of CT and MRI in clinical trials for acute ischemic stroke: current concepts (in Japanese). Jpn J Stroke. 2005;27(4):564–7.
15. Sasaki M, Ida M, Yamada K, Watanabe Y, Matsui M. Standardizing display conditions of diffusion-weighted images using concurrent b0 images: a multi-vendor multi-institutional study. Magn Reson Med Sci. 2007;6(3):133–7.
16. Okuda Y, Suzuki T, Tane K, Ogawa R, Takase T, Inoue T, Fumoto Y, Ikenaga T, Nakata T. Characteristics and outcomes of intracerebral hemorrhage from a hospital in Osaka, Japan (in Japanese). Neurosurg Emerg. 2008;13(1):63–71.
17. Nagashima H, Harakawa T, Doi K. Computerized scheme for automated adjustment of display grayscale in brain diffusion-weighted magnetic resonance images based on density histogram analysis (in Japanese). J Inst Image Inf Telev Eng. 2010;64(6): 874–80.
18. Otsu N. A threshold selection method from gray-level histograms. IEEE Trans Syst Man Cybern. 1979;9(1):62–6.
19. Sener RN, Diffusion MRI. Apparent diffusion coefficient (ADC) values in the normal brain and a classification of brain disorders based on ADC values. Comput Med Imaging Graph. 2001;25(4): 299–326.
20. Nagashima H, Harakawa T. Computer-aided diagnostic scheme for detection of acute cerebral infarctions on brain CT images. J Signal Process. 2008;12(1):73–80.
21. Armato SG 3rd, Giger ML, Chen CT, Vyborny CJ, Ryan J, MacMahon H. Automated registration of frontal and lateral radionuclide lung scans with digital chest radiographs. Acad Radiol. 2000;7(7):530–9.
22. Yamamoto M, Ishida T, Kawashita I, Kagemoto M, Fujikawa K, Mitogawa Y, Ubagai T, Ishine M, Ito K, Akiyama M. Development of computer-aided diagnostic system for detection of lung nodules in three-dimensional computed tomography images (in Japanese). Jpn J Radiol Technol. 2006;62(4):555–64.
23. Nitta S, Hontani H, Fukami T, Yuasa T, Akatsuka T, Wu J, Takeda T, Oriuchi N, Endo K, Watanabe Y. PET/CT image processing for aiding a follow-up of a treatment of lung tumors (PET/CT) (in Japanese). Inst Electron Inf Commun Eng Tech Rep. 2008;107(461):319–24.
24. Sasaki M, Yamada K, Watanabe Y, Matsui M, Ida M. Reliability of diffusion-weighted imaging in acute ischemic stroke: a multi-institutional multivendor validation study (in Japanese). Jpn J Stroke. 2006;28:511–3.
25. Uluğ AM, Beauchamp N Jr, Bryan RN, van Zijl PC. Absolute quantitation of diffusion constants in human stroke. Stroke. 1997;28(3):483–90.
26. Latchaw RE, Yonas H, Hunter GJ, Yuh WT, Ueda T, Sorensen AG, Sunshine JL, Biller J, Wechsler L, Higashida R, Hademenos G. Guidelines and recommendations for perfusion imaging in cerebral ischemia: a scientific statement for healthcare professionals by the writing group on perfusion imaging, from the Council on Cardiovascular Radiology of the American Heart Association. Stroke. 2003;34(4):1084–104.